Asian Journal of Chemistry; Vol. 36, No. 7 (2024), 1549-1558

ASIAN JOURNAL OF CHEMISTRY

https://doi.org/10.14233/ajchem.2024.31646

Synthesis, Characterization and Applications of Some Lanthanide(III) Complexes with Schiff Base Derived from L-Valine and Vanillin

B. SHYNI, J.P. REMIYA and T.S. SIKHA*

Department of Chemistry, Mahatma Gandhi College, University of Kerala, Thiruvananthapuram-695004, India

*Corresponding author: E-mail: drsikhadinesh@gmail.com

Received: 4 April 2024; *Accepted*: 4 May 2024; *Published online*: 29 June 2024; AJC-21674

Three lanthanide complexes of Sm(III), Nd(III) and Dy(III) with Schiff base ligand, potassium 2-((4-hydroxy-3-methoxybenzylidene)amino)-3-methylbutanoate derived from the condensation of vanillin and L-valine have been successfully synthesized by solid-state method. The elemental analysis, and spectral studies, such as CHN analysis, FT-IR & FIR, UV-Visible, HR-MS, TG/DTG analysis, photoluminescent spectra and conductivity measurements, were employed for the comprehensive characterization of these compounds. These data indicate that the synthesized Schiff base ligand act as tridentate (ONO) manner towards the metal ions. Additionally, diverse biological activities such as antimicrobial, antioxidant, antidiabetic, anti-inflammatory and larvicidal activities of the ligand and its lanthanide(III) complexes were analyzed.

Keywords: Photoluminescent spectra, Thermal decomposition, Biological activities, Larvicidal activity.

INTRODUCTION

Schiff base ligand with donor atom (O, N or S) suitable for coordinating with metals have attracted significant research interest in the field. These Schiff bases have been thoroughly explored in transition and non-transition metal/ions to enhance potential biological features [1-3]. Schiff bases derived from amino acids exhibit high efficacy as metal chelating agents, finding various applications in the food and dye industry, analytical chemistry and catalysis. Additionally, the metal complexes formed by amino acids hold substantial potential across in various fields, biological, pharmaceutical and industrial applications, among others [4-7]. In addition to their unique properties, simplicity of manufacturing, chelating properties and stability of compounds that shield metal ions having an azomethine linkage which is important and investigated in various fields of chemistry.

Currently, various Schiff base complexes of lanthanides have demonstrated catalytic activity in polymerization reactions [8,9]. Photoluminescence studies of metal complexes involve investigating the emission of light by coordination compounds containing lanthanide ions. Some lanthanide complexes have distinctive luminous qualities; in particular, Sm(III) complexes exhibit intriguing luminescent capabilities that are emissive in the visible 400-800 nm range of the spectrum [10]. Ligands exert a pivotal influence on the energy levels and emission characteristics of lanthanide(III) complexes, shaping their spectroscopic behaviour. Researchers often engage in ligand design to optimize the luminescence, stability and other characteristics of lanthanide complexes for applications in fields such as optoelectronics, sensing, light emission diodes, fluorescent lighting, luminescence sensors, liquid crystal technologies and biomedical imaging applications. Additionally, the lanthanides are found to possess the coordination numbers and geometries. The paramount significance of coordination compounds of rare earths in cancer treatment and diagnosis stems from the potential exploitation of paramagnetic properties exhibited by lanthanides and their compounds. These compounds are generally used in medicine as MRI contrast media [11].

The luminescent intensities of the lanthanide complexes are intricately linked to the organic ligand ability to efficiently absorb UV light, facilitate energy transfer from the ligand to metal and the effectiveness of lanthanide metal luminescence, as highlighted in previous studies [12,13]. Moreover, these complexes demonstrate noteworthy luminescent properties,

such as quantum yield, molar extinction coefficient, extended fluorescence lifespan and significant stokes shifts [14].

The synthesis of numerous lanthanide(III) complexes, conducted in solution state and the solid state, acquiring remarkable importance attributed to their significant biological activities. A review of the literature reveals that the number of studies on the solid-state synthesis of lanthanide(III) complexes with vanillin is very limited. In current study, we describe three lanthanide(III) complexes formed with the Schiff base ligand derived from vanillin and L-valine amino acid, in solid state.

EXPERIMENTAL

Analytical grade chemicals were utilized in this investigation. Sm(III), Nd(III), Dy(III) chloride hexahydrate, L-valine, Vanillin (Sigma-Aldrich) and KOH (Merck) were employed for the synthesis without further purification. Spectroscopic grade reagents were used for the spectral studies.

Physical measurements: By using Perkin-Elmer 2400 CHNO elemental analyzer, C, H, N and O analysis of the compounds were analyzed. FT-IR spectrum was documented covering the spectral range of 4000-400 cm^{-1} (KBr disks) on Perkin-Elmer C96217 model spectrophotometer. The FAR-IR spectrum of the Ln(III) complexes was obtained using a 3000 Hyperion Microscope with Vertex 80 FTIR System within the range of 500-30 cm^{-1}. Electronic spectrum was determined by utilizing Perkin-Elmer Lambda-25 UV-Visible spectrophotometer within the run of 200-800 nm in the solid state, employing KBr disks. ^{1}H NMR spectra was determined by utilizing a Bruker-Avance III HD 400 MHz One Bay FT NMR spectrometer. The photoluminescence (PL) spectrum was captured using a sophisticated Fluorescence Spectrometer, FLS 1000, spanning the range of 200-800 nm. TG/DTG analysis was employed to determine simultaneous thermal analyzer. Mass spectrometry was performed using the HRMS spectrophotometer in the HREMI Thermo-Scientific Exactive System. Conductivity measurements were recorded at 298 K in DMSO solvent (10^{-3} M) using the Systonic Model 303 conductivity meter. The magnetic measurements were conducted on a Sherwood Scientific Gouy Balance and the melting points were determined using an Analab melting point apparatus.

Synthesis of Schiff base ligand K(val-van): The Schiff base ligand was synthesized through the condensation of vanillin and L-valine as reported in earlier procedures [15,16]. The equimolar ratio of valine with vanillin and KOH were weighed, put in an agate and then thoroughly grinded until the mixture became sticky form. The reactant's colour changed yellow and took around 30 min a solid powder was obtained. The products were washed with a small amount of cold dehydrated ethanol and subjected to recrystallization in hot ethanol. Following this, the products were dried in a vacuum drying oven at 40 ºC.

K(val-van): Yellow solid; m.p.: 94 ºC; yield 88%. Anal. calcd. (found) % of $KC_{13}H_{16}O_4N$: C, 53.99 (52.38); H, 5.53 (5.18); N, 4.84 (4.42); O, 22.11 (21.89). IR: (KBr, λ_{max}, cm^{-1}): 3165 ν(O-H), 1660 ν(C=N), 1586 $\nu_{as}(COO)^-$, 1334 $\nu_s(COO)^-$, 1270 ν(C-O); ^{1}H NMR (500 MHz, CH_3OH, δ ppm): 3.95 (3H, s, –OCH_3), 7.59 (1H, s, HC=N), 7.01-7.43 (m, 6H, ArH). 4.5–5.0 (1H, S, CH_3), 9.817 (1H, s, OH). ESI-MS (*m/z*): 289.37; UV-Vis (λ_{max}, nm): 226, 284, 400, 512.

Synthesis of lanthanide(III) complexes: In an agate mortar, corresponding lanthanide(III) chloride (5 mmol) was added to Schiff base ligand (5 mmol) and ground for 45 min. The solid products obtained was filtered off, washed with dehydrated ethanol and distilled water several times and dried in a vacuum drying oven at 70 ºC for roughly 72 h (**Scheme-I**).

[Sm(val-van)$_2$(H_2O)$_3$Cl]·H_2O (1): Yellow solid; yield: 76%; m.p.: 255 ºC; molar conductance: 10 Ω^{-1} cm^2 mol^{-1}; μ_{eff}: 1.60 B.M. Anal. calcd. (found)% for $SmC_{26}H_{38}O_{12}N_2Cl$: C, 41.24 (41.28); H, 4.98 (5.02); N, 3.60 (3.70); O, 25.35 (25.40); Sm, 19.89 (19.87). IR: (KBr, λ_{max}, cm^{-1}): 3356 ν(H_2O), 1656 ν(C=N), 1580, $\nu_{as}(COO)^-$; 1309, $\nu_s(COO)^-$; 1232, ν(C-O); 432, ν(M-N), 369, ν(M-O), 316, ν(M-Cl), ESI-MS (*m/z*): 755.81; UV-Vis (λ_{max}, nm): 235, 300, 393.

[Nd(val-van)$_2$(H_2O)$_3$Cl]·H_2O (2): Light violet; yield: 76%, m.p.: 250 ºC; molar conductance: 12 Ω^{-1} cm^2 mol^{-1}; μ_{eff}: 3.60 B.M. Anal. calcd. (found)% for $NdC_{26}H_{38}O_{12}N_2Cl$: C, 41.55 (41.61); H, 4.83 (5.06); N, 3.66 (3.73); O, 25.44 (25.61); Nd, 19.23 (18.20). IR (KBr, λ_{max}, cm^{-1}): 3223 ν(H_2O), 1642 ν(C=N), 1582 $\nu_{as}(COO)^-$, 1310 $\nu_s(COO)^-$, 1229 ν(C-O), 425 ν(M-N), 350 ν(M-O), 312 ν(M-Cl); ^{1} H NMR (500 MHz, DMSO, δ ppm): 3.972 (s, 3H, OCH_3), 4.963 (s, 1H, HC=N), 6.645-7.669 (m, 6H, ArH); ESI-MS (*m/z*): 749.81; UV-Vis (λ_{max}, nm): 244, 345, 523, 580, 743, 800.

[Dy(val-van)$_2$(H_2O)$_3$Cl]·H_2O (3): Yellow solid; yield: 78%, m.p.: 240 ºC; molar conductance: 10.05 Ω^{-1} cm^2 mol^{-1}; μ_{eff}: 10.00 B.M. Anal. calcd. (found)% for $DyC_{26}H_{38}O_{12}N_2Cl$: C, 40.55 (40.62); H, 4.82 (4.94); N, 3.58 (3.64); O, 24.89 (25.00); Dy, 21.10 (21.16). IR (KBr, λ_{max}, cm^{-1}): 3351 ν(H_2O), 1651 ν(C=N), 1582 $\nu_{as}(COO)^-$, 1309 $\nu_s(COO)^-$, 1220 ν(C-O), 468 ν(M-N), 363 ν(M-O), 318 ν(M-Cl); ESI-MS (*m/z*): 767.95; UV-Vis (λ_{max}, nm): 242, 344, 392.

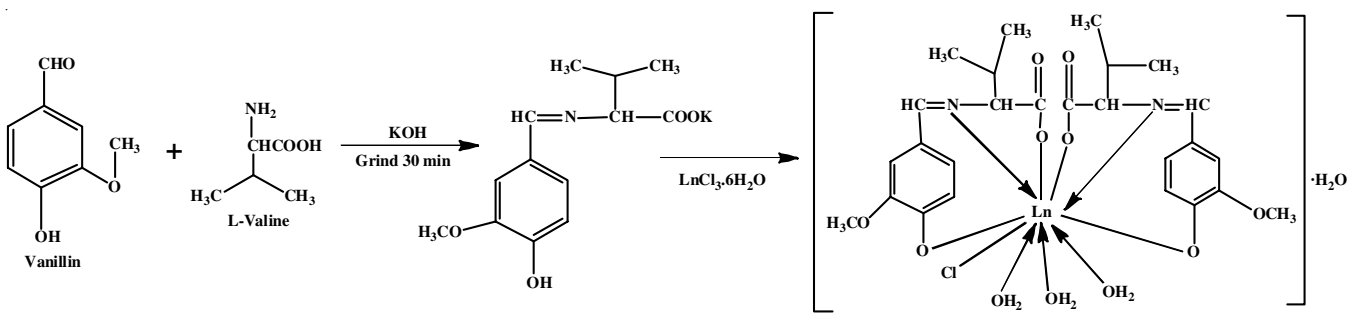

Scheme-I: The possible structure of the lanthanide complexes [Ln(val-van)$_2$(H_2O)$_3$Cl]·H_2O; where, Ln = Sm, Nd and Dy

Antimicrobial studies: The antibacterial activity of the Schiff base ligand and its lanthanide(III) complexes was investigated against two bacterial strains (*Escherichia coli*, *Staphylococcus aureus*). The antifungal activity was assessed against two pathogenic fungal strains (*Aspergillus niger*, *Rhizopus*) using the Agar well diffusion method. Mueller-Hinton Agar was utilized to evaluate the antimicrobial activity of the compounds. All samples were dissolved in 100% DMSO to achieve a final concentration of 20 µg/mL. The samples were loaded into the wells and the activity was analyzed. Amikacin and nystatin were used as positive standards for antibacterial and antifungal studies, respectively, while DMSO served as the negative control. All plates were incubated for 24 h at 37 ºC and the zone of inhibition around the disc was measured in millimeters (mm).

Antioxidant activity assay: The antioxidant activity of the Schiff base ligand and its lanthanide(III) complexes, as well as the standard, was evaluated based on the radical scavenging effect using 1,1-diphenyl-2-picryl-hydrazyl (DPPH) method. This method is one of the simplest approaches for calculating free radical scavenging activities. Prior to UV measurements, a methanolic solution of DPPH (60 µM) was prepared and 3.9 mL of solution was mixed with varying concentrations of the methanol compound mixture (25, 50, 75 and 100 µg/mL). The samples were kept in the dark for 15 min at room temperature and the decrease in absorbance was measured at 515 nm using a UV-Vis spectrophotometer. The experiment was conducted in triplicate, with a control sample prepared containing the same volume without any extract and reference ascorbic acid was included. A 95% methanol solution was used as the blank. Ascorbic acid, dissolved in distilled water to create a stock solution with a concentration of (1 µg/100 µL), served as the reference standard. Radical scavenging activity was calculated by the following formula:

$$\text{Inhibition } (\%) = \frac{A_{\text{control}} \text{ at } 0 \text{ min} - A_{\text{test}}}{A_{\text{control}} \text{ at } 15 \text{ min}} \times 100$$

Anti-inflammatory activity: Reaction mixture (0. 5 mL) consisted of test compounds and an aqueous solution of 0.45 mL BSA (3%) and varying concentration of compounds (25, 50, 75, 100 mg/mL) pH was adjusted to 6.3 using small amount of 1 N HCl. The samples were incubated at 37 ºC for 20 min. and then heated at 80 ºC for 2 min. After cooling the samples, 2.5 mL phosphate buffer saline (pH-6.3) was added to each tube. The absorbance was measured using a spectrophotometer at 416 nm. The percentage inhibition of protein denaturation was calculated as follows:

$$\text{Inhibition } (\%) = \frac{A_{\text{control}} - A_{\text{sample}}}{A_{\text{control}}} \times 100$$

Antidiabetic activity: The reducing sugars produced by the action of α-amylase react with dinitrosalicylic acid, reducing it to a brown-coloured product, nitro amino salicylic acid. Different concentrations of the sample, ranging 12.5 to 200 µg/mL, were prepared from a stock concentration of 1 mg/mL and made up to 1000 µL using 25 mM phosphate buffer at pH 6.9. This solution also contained 25 µL of porcine α-amylase at a concentration of 0.5 mg/mL. The mixtures were incubated at 25 ºC for 10 min. After pre-incubation, 25 µL of 0.5% starch solution in 25 mM phosphate buffer at pH 6.9 was added. The reaction mixtures were further incubated at 25 ºC for 10 min. The reaction was stopped by adding 50 µL of 96 mM 3,5-dinitrosalicylic acid colour reagent. The microplate was then incubated in a boiling water bath for 5 min and cooled to room temperature. Absorbance was measured at 540 nm using a microplate reader (Erba, Lisascan) and acarbose was used as the standard drug.

Larvicidal activity: Mosquito larvae were collected from water habitats in Nagercoil city, India using a wide-mouth container. The mosquito samples were then brought to the laboratory, morphologically identified using standard manual methods and utilized for larvicidal activity studies. Cleaned sterile beakers were selected and 20 early instar larvae of Culex were placed in 100 mL of tap water. To this, 100 ppm of synthesized compounds was added. A control group consisting of 20 larvae in tap water (without compounds) was also prepared. The beakers were left undisturbed for 24, 48, 72 and 96 h to observe the mortality of the Culex larvae.

RESULTS AND DISCUSSION

The comparison of experimental and calculated elemental percentages reveals a strong agreement, affirming the stoichiometry of the synthesized compounds. All the synthesized three lanthanide(III) complexes exhibit a 1:2 (M:L) stoichiometry. They demonstrate solubility in DMSO, springly solubility in ethanol and methanol and insolubility in acetone, chloroform and distilled H_2O.

Molar conductivity: The conductance data of the lanthanide(III) complexes were found to be within the range of 10.00-12.00 Ω^{-1} cm^2 mol^{-1}. These findings suggest the lanthanide(III) complexes are non-electrolytic and the chloride ion is present within the coordination sphere.

Magnetic moment: Measurements for determining the magnetic susceptibility values of the lanthanide(III) complexes were conducted to elucidate the exact structure. The obtained effective moments of Ln(III) complexes were 1.60, 3.60 and 10.00 B.M. for Ln = Sm^{3+}, Nd^{3+} and Dy^{3+}, respectively, providing the strong support for the proposed structures [17,18]. In these complexes, the magnetic moments are not affected by the ligand field, suggesting that the 4*f* electrons do not take part in bond formation [19,20].

IR spectral studies: The Schiff base ligand shows a strong band at 1660 cm^{-1} which attributed to the stretching vibration of azomethine group (-HC=N), these bands was shifted to lower frequencies on complexation 1656-1642 cm^{-1}, indicating that azomethine nitrogen coordinated to the metal ions [21]. The asymmetric and symmetric stretching frequency of carboxylate (COO^-) group of the ligand appears as a strong band at 1586 cm^{-1} and a weak band at 1334 cm^{-1} (Fig. 1). These bands are shifted around 1582-1580 cm^{-1} and 1310-1309 cm^{-1} during complexation, the $\Delta\nu$ (> 250 cm^{-1}) suggested the unidentate coordination of the carboxylate with Ln(III) ion. Furthermore, the phenolic C-O stretching vibration, observed at 1270 cm^{-1} in the Schiff base ligands, exhibited a significant shift to the lower frequency range of 1237-1220 cm^{-1} upon coordination, confirming the coordination of the ligand to the metal ion in

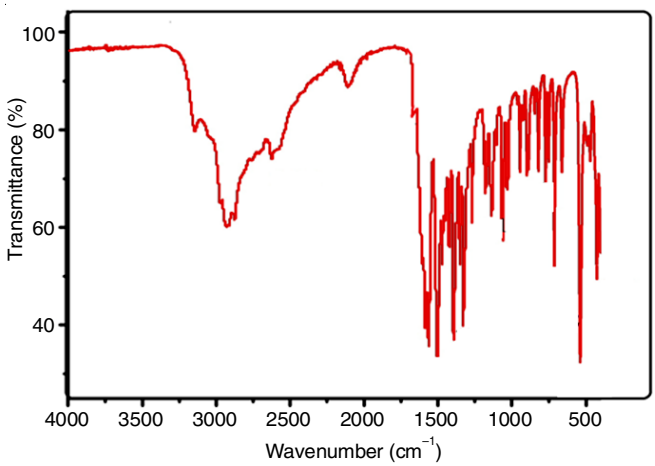

Fig. 1. FT- IR spectrum of Schiff base ligand; K(val-van)

the corresponding metal chelates. Spectral bands in the range 3356-3223 cm^{-1} for ν(O-H) were assigned to water molecules present in the complexes, which are in agreement with mass and thermal results [22-25]. The coordination mode of Schiff base ligands was further supported by the new frequencies occurring in the Far-infrared spectra of Sm(III), Nd(III) and Dy(III) complexes. In the lower frequency region, the Far-IR bands at 432, 425 and 468 cm^{-1} arise due to ν(M-N) and 369, 350 and 363 cm^{-1} arise due to ν(Ln-O) and 316, 312 and 318 cm^{-1} ν(M-Cl) frequencies, respectively [26,27]. From the spectra, it may be concluded that these Ln(III) complexes have almost similar structure and the Schiff base ligand coordinates with the metal ion in tridentate manner. The spectra of the synthesized Sm(III) complex are given in Fig. 2.

UV-Vis spectral studies: The electronic absorption spectra of the Schiff base and its Ln(III) complexes are shown in Table-1. The Schiff base ligand was characterized by four main bands at 226, 284, 400 and 512 nm, which can be attributed to the π–π* and n–π* of benzene ring and azomethine group, respectively (Fig. 3). The spectra of the Ln(III) complexes typically exhibit the characteristic bands of Schiff base ligand, displaying alterations in both frequencies and intensities. These shifts and changes in absorption band intensities are indicative of the coordination of Schiff base ligands to the metal center.

TABLE-1
UV-VISIBLE SPECTRAL DATA OF THE SCHIFF BASE LIGAND AND ITS LANTHANIDE COMPLEXES

Compounds	λ_{max} (nm)	Band assignments
Schiff base Ligand; K(val-van)	226	π→π*
	284	π→π*
	400	n→π*
	512	n→π*
$[Sm(val\text{-}van)_2(H_2O)_3Cl]\cdot H_2O$	235	π→π*
	300	LMCT
	393	n→π*
$[Nd(val\text{-}van)_2(H_2O)_3Cl]\cdot H_2O$	244	π→π*
	345	n→π*
	523, 580	$^4I_{9/2}\rightarrow{}^4G_{7/2}$, $^4G_{5/2}$
	743, 800	$^4I_{9/2}\rightarrow{}^4F_{7/2}$
$[Dy(val\text{-}van)_2(H_2O)_3Cl]\cdot H_2O$	242	π→π*
	344	LMCT
	392	n→π*

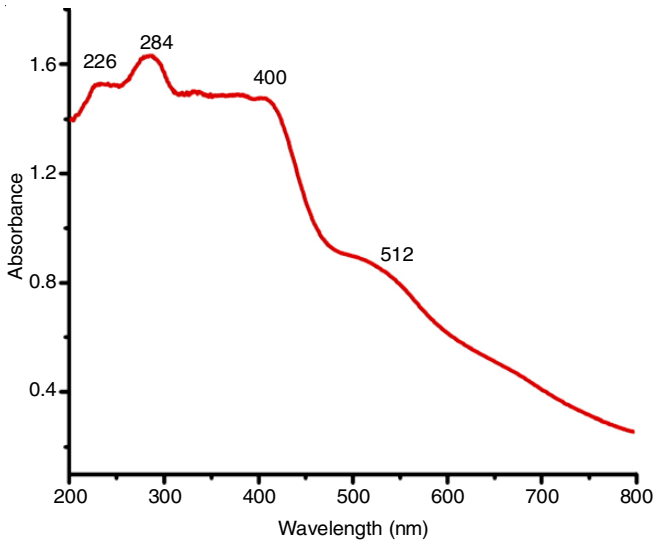

Fig. 3. UV-Vis spectrum of Schiff base ligand; K(val-van)

The absorption bands of the Sm(III) complex exhibit a slight red shift to lower frequencies at transitions around 235, 300 and 393 nm. The emergence of a new band at approximately 300 nm provides additional evidence for complex formation.

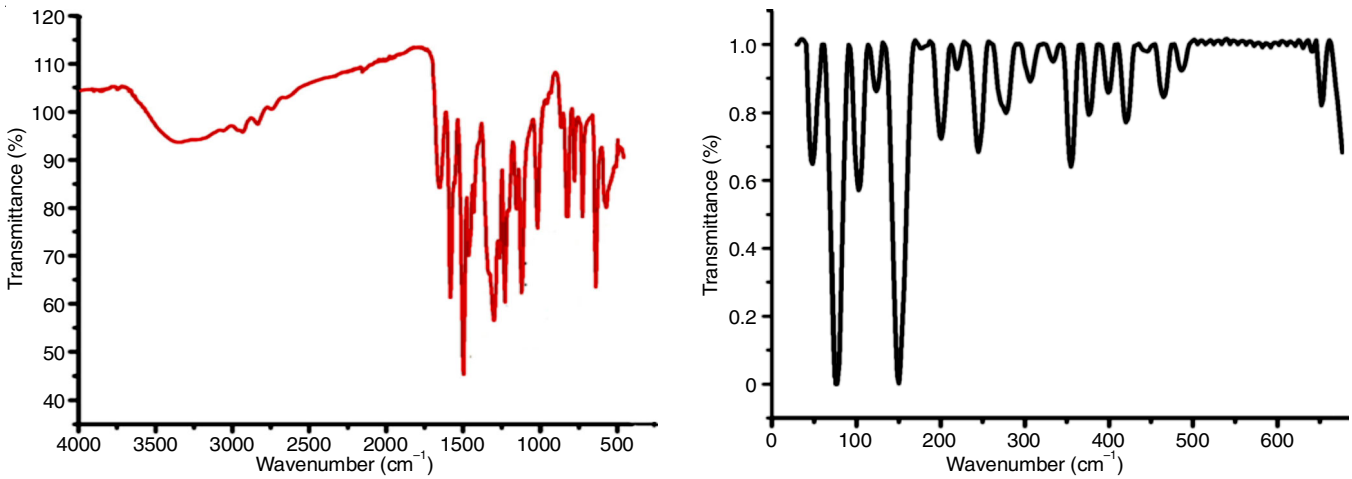

Fig. 2. FT-IR and FIR spectra of $[Sm(val\text{-}van)_2(H_2O)_3Cl]\cdot H_2O$

The 300 nm band is assigned to the LMCT transfer, while the band around 393 nm may be attributed to the π–π* transition state of the azomethine coupled with charge transfer from the ligand to the metal (Fig. 4). Similarly, the Nd(III) complex display the transitions at 244, 345 and 523 nm, also the lower intensity bands at 580 ($^4I_{9/2}\rightarrow{}^4G_{7/2,}{}^4G_{5/2}$) and 743, 798 ($^4I_{9/2}\rightarrow{}^4F_{7/2}$) nm. The Dy(III) complex shows at 242, 344 and 392 nm transitions (Fig. 5) [28,29]. The lanthanide ions do not appreciably contribute to the spectra of their complexes since *f–f* transitions are Laporte forbidden and very weak.

Band gap measurement: The band gap is of fundamental importance of the complexes were calculated from the UV-Vis spectra [30,31]. The absorbance was employed to approximately calculate the absorption coefficient (α) by using the relation;

$$\alpha = \frac{1}{d}\ln A \quad (1)$$

The optical band gap (E_g) was calculated from the relation;

$$\alpha h\nu = A\,(h\nu - E_g)^m \quad (2)$$

where m is equal to (1/2 and 2) direct and indirect transitions, respectively. The direct band gap values were 2.75 (calcd. 2.51), 2.64 (calcd. 2.53) and 2.69 (calcd. 2.51) eV for Sm(III), Nd(III) and Dy(III) complexes, respectively. The absorption data reveals the direct transition of the complexes of semi-conducting in nature.

Photoluminescence studies: The luminescent property of Schiff base ligand and its Ln(III) complexes were explored through fluorescence spectra recorded in the solid state. The emission spectrum was recorded with excitation at 320 nm and the Schiff base ligand exhibits a fluorescence band at 412 nm attributed to π–π^* transition (Fig. 6a). The emission spectrum of Sm(III) complex was recorded upon excitation at 380 nm, revealing luminescence bands corresponding to $^4I_{9/2}\rightarrow{}^4G_{9/2}$

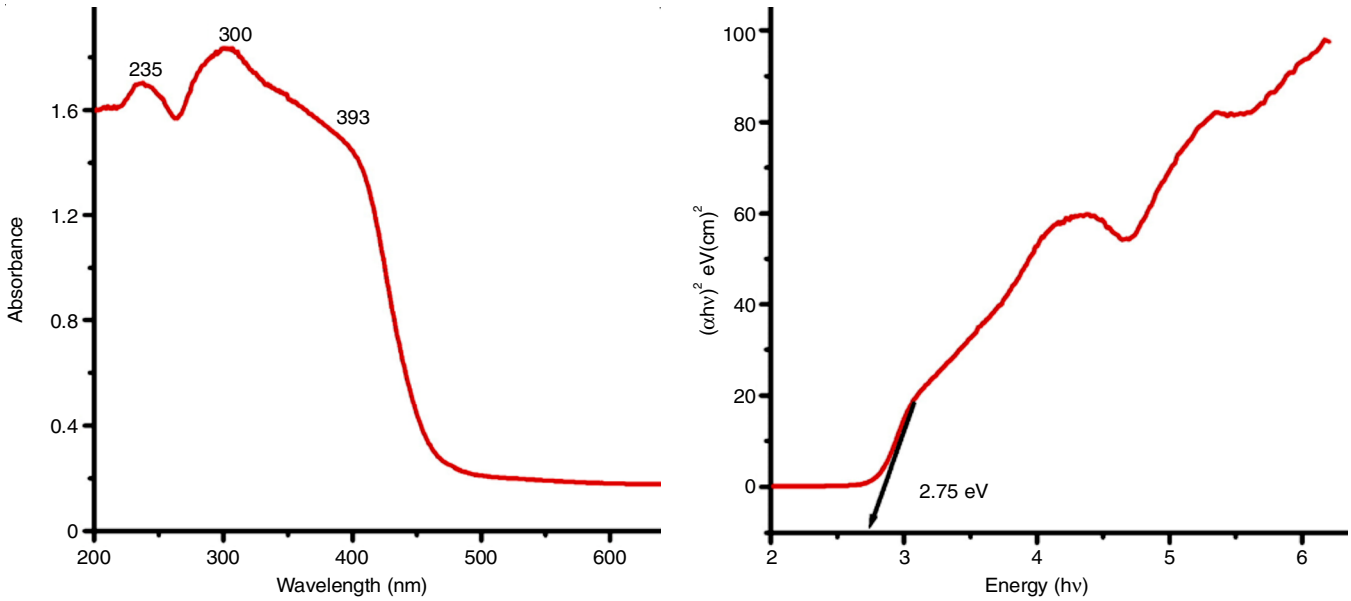

Fig. 4. UV-Vis spectrum and Tauc's plot of $[Sm(val\text{-}van)_2(H_2O)_3Cl]\cdot H_2O$

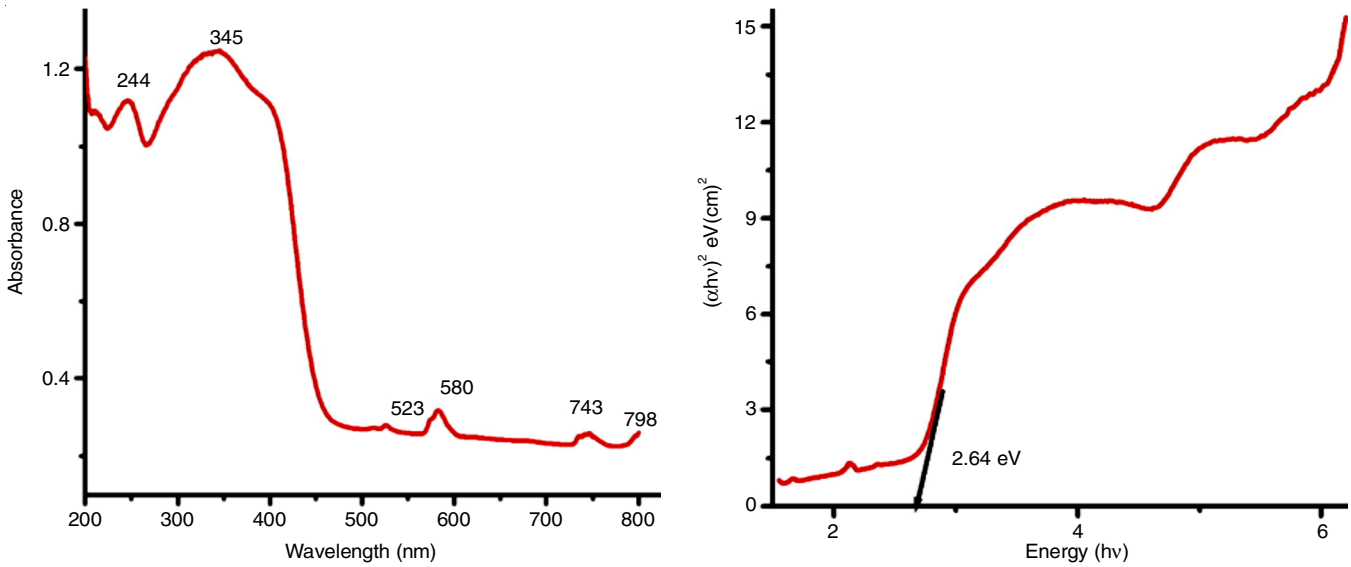

Fig. 5. UV-Vis spectrum and Tauc's plot of $[Nd(val\text{-}van)_2(H_2O)_3Cl]\cdot H_2O$

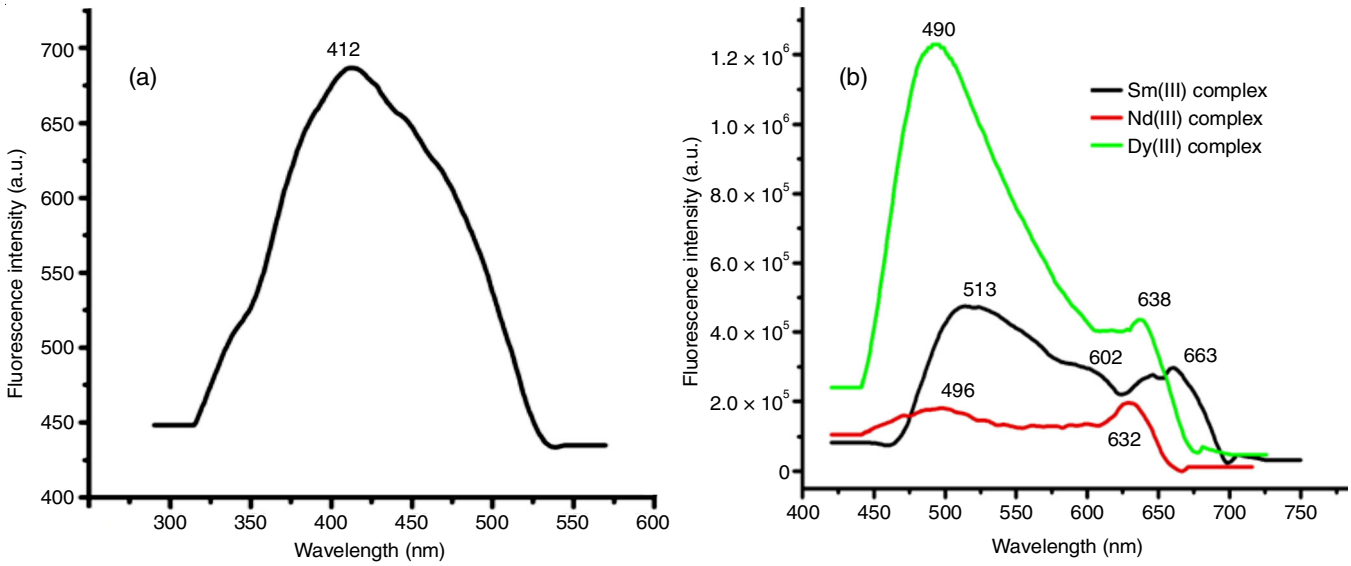

Fig. 6. Emission spectrum of (a) Schiff base ligand; K(val-van) and (b) $[Ln(val\text{-}van)_2(H_2O)_3Cl]\cdot H_2O$; where, Ln = Sm, Nd and Dy

(513) and $^4I_{9/2}\rightarrow{}^2H_{11/2}$ (602, 663) nm electronic transitions. It exhibited sharp emission bands resulting from *f–f* transitions of the samarium ion (Fig. 6b). Similarly, the Nd(III) complex, recorded upon excitation at 390 nm, displayed luminescence bands corresponding to $^4I_{9/2}\rightarrow{}^4G_{11/2}$ (496) and $^4I_{9/2}\rightarrow{}^2H_{11/2}$ (632) nm transitions, respectively [18,32]. Under the excitation, the Nd(III) complex exhibited characteristic fluorescent property (Fig. 6b). The Dy(III) complex, recorded upon excitation at 390 nm, exhibited characteristic emission peaks arising from $^4F_{9/2}\rightarrow{}^6H_{15/2}$ (490) and $^4F_{9/2}\rightarrow{}^6H_{11/2}$ (638) nm transitions (Fig. 6b). Based on these results, these complexes are excellent candidates for potential fluorescence applications [33,34].

^{1}H NMR spectral studies: The NMR spectrum of the ligand was taken in methanol at room temperature. The Schiff base ligand exhibited a signal at δ 3.95 ppm is attributed to the 3H singlet of the (–OCH_3) group. The peak at δ 7.59 ppm was assigned to the azomethine proton, HC=N, 1H singlet. As the molecule contains an aromatic ring, the multiple signals between δ 7.01-7.43 ppm were assigned to the aromatic ring proton resonances. The peak for CH_3 protons was observed at δ 4.5-5.0 ppm in the Schiff base ligand, corresponding to methyl protons. The hydroxyl proton appeared at δ 9.817 ppm as a singlet [35,36]. In the NMR spectrum of Nd(III) complex, the disappearance of the (-OH) peak and the shift of the aromatic peak to a higher value confirm the formation of the complex. The signals at δ 3.972 ppm (singlet, 3H, OCH_3), δ 4.963 ppm (singlet, 1H, HC=N) and the range of δ 6.645-7.669 ppm (multiplet, 6H, ArH) are attributed to the aromatic protons [37].

Mass spectral studies: The spectrum of Schiff base had a prominent molecular ion $[KC_{13}H_{16}O_4N]$, *m/z* = 293.15 $[M+4H]^+$; [calcd. 289.15] a.m.u confirming the molecular weight of Schiff base ligand. The base peaks at *m/z* = 206, which corresponds to the fragment $[C_{13}H_4NO_2]$ and other important peaks 137 and 252 are due to the loss of $[C_7H_7NO_2]$, $[KC_{11}H_3NO_4]$ and fragments from the parent molecule [38,39]. The spectrum of the samarium(III) complex confirms the stoichiometry of the complex $[Sm(val\text{-}van)_2(H_2O)_3Cl]\cdot H_2O$, with the base peak at *m/z* = 120.08, indicating the loss of $[C_4H_{10}NO_3]$. Other important peaks were 124, 169, 185, 199, 254, 300, 319, 351, 439, 457, 473, 573, 683, 720 and 755. The molecular ion peak at *m/z* = [755.14], [calcd. 755.81] a.m.u. which is equivalent to its molecular weight.

The spectra of $[Nd(val\text{-}van)_2(H_2O)_3Cl]\cdot H_2O$ shows the base peak at *m/z* = 331 was due to the loss of $[C_{14}H_7N_2O_8]$. Other important peaks are 154, 162, 179, 197, 211, 252, 303, 363, 409, 457, 549, 645, 734 and 773. The molecular ion peak at *m/z* = [773.14+ Na+2H]$^+$ [calculated = 749.81] a.m.u. which is equivalent to its molecular weight.

The mass spectra of $[Dy(val\text{-}van)_2(H_2O)_3Cl]\cdot H_2O$ shows the base peak at *m/z* = 309 was due to the loss of $[C_{14}H_{17}N_2O_6]$. Other important peaks were 157, 161, 165, 189, 231, 235, 253, 313, 317, 341, 415, 512, 590, 694 and 792. The molecular ion peak at *m/z* [792.71+Na+2H]$^+$ [calculated = 767.95] a.m.u. which is equivalent to its molecular weight. The coordination of water molecules were identified in the mass spectra of Sm(III), Nd(III) and Dy(III) complexes. The mass fragmentation and analytical results matched to the stoichiometric ratio of the synthesized complexes.

Thermal studies: The synthesized Ln(III) complexes were subjected to thermogravimetry (TG) and derivative thermogravimetry (DTG) under a N_2 environment. This approach was employed to analyze their thermal behaviour, including aspects such as thermal stabilities and decomposition stages. The suggested stepwise thermal degradation patterns, detailing the temperature-dependent decomposition and the formation of respective metal oxides are outlined in Table-2. All the lanthanide (III) complexes show almost the same type of decompositions stages resulting in the formation of metal oxide [40,41].

$[Sm(val\text{-}van)_2(H_2O)_3Cl]\cdot H_2O$ (1): TG/DTG studies show that Sm(III) complex undergoes thermal decomposition in three stages (Fig. 7a). In first stage, the loss of one lattice water molecule takes place in the temperature range 50-115 ºC with weight loss of 2.30% (calcd. 2.38%). The second stage decomposition occurs in the temperature range 120-220 ºC with an

TABLE-2
THERMOGRAVIMETRIC DATA OF THE COMPLEXES

Compounds	Decomp. stages	Temp. range (°C)	Mass. loss% (calcd. found)	Probable assignments
$[Sm(val\text{-}van)_2(H_2O)_3Cl]\cdot H_2O$	I	50-115	2.30/2.38	Loss of one lattice water
	II	120-220	7.14/7.06	Loss of three coordinated water
	III	220-685	70.91/70.59	Loss of organic moieties and chlorine, formation of Sm_2O_3
$[Nd(val\text{-}van)_2(H_2O)_3Cl]\cdot H_2O$	I	50-110	2.40/2.38	Loss of one lattice water
	II	120-245	7.20/7.00	Loss of three coordinated water
	III	246-690	71.49/71.40	Loss of organic moieties and chlorine, formation of Nd_2O_3
$[Dy(val\text{-}van)_2(H_2O)_3Cl]\cdot H_2O$	I	52-110	2.34/2.32	Loss of one lattice water
	II	115-255	7.03/7.00	Loss of three coordinated water
	III	257-680	69.79/69.70	Loss of organic moieties and chlorine, formation of Dy_2O_3

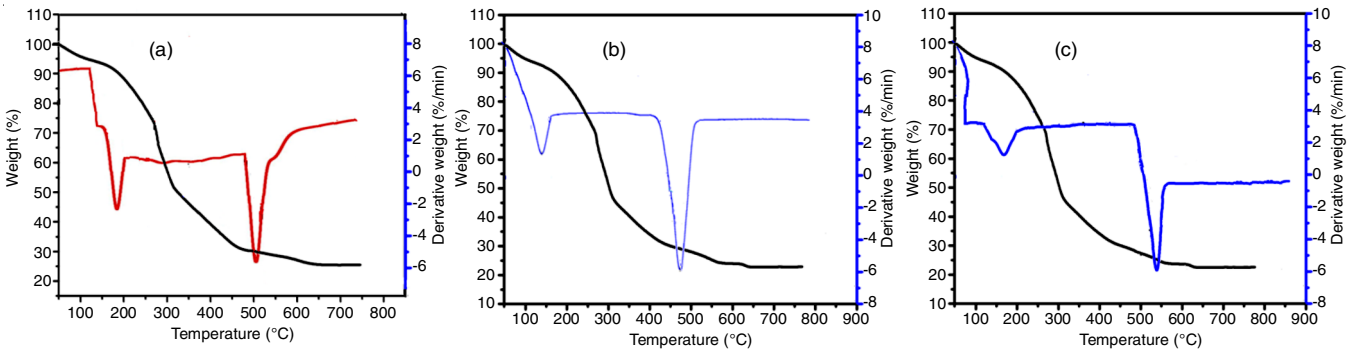

Fig. 7. TG/DTG curves of (a) $[Sm(val\text{-}van)_2(H_2O)_3Cl]\cdot H_2O$, (b) $[Nd(val\text{-}van)_2(H_2O)_3Cl]\cdot H_2O$ and (c) $[Dy(val\text{-}van)_2(H_2O)_3Cl]\cdot H_2O$

observed weight loss of 7.06% (calcd. 7.14%), which corresponds to the removal of three coordinated water molecules. The third stage of decomposition occurred at the temperature range from 220-685 ºC, with weight loss of 70.59% (calcd. 70.91%), which corresponds to the loss of two organic moieties and chlorine and the formation of stable oxide.

$[Nd(val\text{-}van)_2(H_2O)_3Cl]\cdot H_2O$ (2): In Nd(III) complex, the first stage of decomposition started at 50 ºC and completed at 118 ºC; the mass loss corresponding to one mole of lattice water per mole of the complex (weight loss found 2.40%; calculated, 2.38%). Second stage of decomposition occurs in the range 120 to 245 ºC, the mass loss corresponds to three moles of coordinated water per mole of complex (weight loss found 7.20%, calculated, 7.00%). The third stage of decomposition took place in the temperature range from 246 to 690 ºC and the loss of two organic moieties and chlorine (weight loss found, 71.49%; calculated, 71.40%) (Fig. 7b).

$[Dy(val\text{-}van)_2(H_2O)_3Cl]\cdot H_2O$ (3): In Dy(III) complex, the first stage of decomposition started at 52 ºC and completed at 110 ºC. The mass loss was corresponding to one mole of lattice water per mole of complex (weight loss found 4.48%; calculated 4.27%). Second stage of decomposition occurs in the range 115 to 255 ºC. The mass loss corresponds to three moles of coordinated water per mole of complex (weight loss found 7.03%; calculated 7.00%). The third stage of decomposition took place in the temperature range from 257 to 680 ºC and the loss of two organic moieties and chlorine (weight loss found 69.79%; calculated 69.70%) (Fig. 7c).

It suggests that the decomposition of synthesized Ln(III) complexes leads probably to appropriate metal oxide as the final products (Sm_2O_3, Nd_2O_3 and Dy_2O_3). An independent pyrolysis experiment was also carried out for each of the Ln(III) complexes studied and the loss of mass determined in each case was compared with that obtained from TG analysis [42].

Biological assays

Antibacterial activity: The results of the bactericidal and fungicidal investigations for the compounds are summarized in Table-3, employing the well diffusion method. Inhibition zone values (in mm) were measured and compared with the standard. Each compound was DMSO solution, with a reference drug as a positive control and solvent DMSO as a negative control. At concentration of 40 µg/mL, ligand showed a 7 mm zone for *S. aureus*, while the complexes exhibited the highest activity with inhibition zones of 15, 9 and 9 mm, respectively. Similarly, at the same concentration, Schiff base ligand [K(val-van)] displayed a 15 mm inhibition zone for *E. coli* and the Ln(III) complexes demonstrated the highest activity with inhibition zones of 16, 12 and 12 mm, respectively. From the results revealed that at a concentration of 40 µg/mL, Sm(III) complex showed higher activity against Gram-positive bacteria (*S. aureus* and *E. coli*). It is suggested that functional groups such as hydroxyl or azomethine groups in the complexes play a major role in their antibacterial activity. Chelation significantly reduces the polarity of the metal ion through partial sharing of the positive charge with donor groups, allowing for electron delocalization over the entire chelate ring. This chelation-induced increase in lipophilicity facilitates the passage of the core metal atom through the lipid layer of the cell membrane, potentially enhancing the antibacterial property.

TABLE-3
ANTIMICROBIAL ACTIVITY OF THE SCHIFF BASE LIGAND AND ITS LANTHANIDE COMPLEXES

Compounds	Concentration (µg/mL)	Bacterial strains (mm)		Fungal strains (mm)	
		S. aureus	*E. coli*	*A. niger*	*Rhizopus*
Schiff base ligand, K(val-van)	40	7	15	7	7
$[Sm(val\text{-}van)_2(H_2O)_3Cl]\cdot H_2O$	40	15	16	10	10
$[Nd(val\text{-}van)_2(H_2O)_3Cl]\cdot H_2O$	40	9	12	12	15
$[Dy(val\text{-}van)_2(H_2O)_3Cl]\cdot H_2O$	40	9	12	10	12
Standard	40	25	25	25	25

Antifungal activity: The *in vitro* antifungal activity against *A. niger* and *Rhizopus* was investigated for the compounds. At a concentration of 40 µg/mL, the Schiff base ligand exhibited the highest inhibition zone of 7 mm against *A. niger*, surpassing the two complexes Sm and Nd with inhibition zones of 10 and 12 mm, while the Dy(III) complex showed 10 mm. Similarly, against *Rhizopus*, the Schiff base ligand showed the highest inhibition zone of 7 mm compared to the other complexes at 10, 15 and 12 mm. From the results revealed that at concentration of 40 µg/mL, the Nd(III) complex displayed higher activity against fungal strains (*A. niger* and *Rhizopus*) compared to the standard, Schiff base ligand and Ln(III) complexes. Based on their antimicrobial activity against pathogenic microorganisms, all synthesized Ln(III) complexes were found to be more potent than their respective Schiff base ligand. The activity of the complexes is dependent on the ligand's chelation ability, the nature of nitrogen donor ligands, the total charge of the complex, the presence and nature of the metal ion neutralizing the ionic complex and the nuclearity of the metal center in the complex [43-45].

Antioxidant activity: Antioxidant activity of the compounds was studied by the DPPH method, comparing scavenging activities with ascorbic acid. Table-4 details radical scavenging effects at varying concentrations showing increased effects for Ln(III) complexes at 25, 50, 75 and 100 µg/mL. The antioxidant activity was quantified using IC_{50} in this study. The Sm(III) complex was significantly more efficient in quenching DPPH radical than the other complexes and standard [46,47]. The IC_{50} values of Schiff base ligand, Sm(III), Nd(III) and Dy(III) complexes were 2.43, 11.14, 19.17 and 14.15%, respectively. Lanthanide(III) complexes, due to ligand coordination, are more effective free radical scavengers than their corresponding Schiff base ligands. Metal Schiff base antioxidants are currently recognized for safeguarding living systems from oxidative stress or free radicals. Differences in antioxidant activity may be linked to factors like chelate ring size, axial ligation and the degree of unsaturation in the chelate ring, influencing complex redox properties [48,49].

Anti-inflammatory activity: The anti-inflammatory activity of the compounds was assessed by studying their ability to inhibit protein denaturation, specifically heat-induced albumin denaturation. The concentration-dependent analysis revealed that at 25, 50, 75 and 100 µg/mL (Table-5), the Nd(III) complex exhibited significant activity compared to the ligand [50]. In the context of global interest in the role of inflammation in human and animal diseases, synthesizing more potent anti-inflammatory drugs with fewer side effects is crucial.

TABLE-4
ANTIOXIDANT ACTIVITY OF SCHIFF BASE LIGAND AND ITS LANTHANIDE COMPLEXES

Compounds	Conc. (µg/mL)	OD at 515 nm	Inhibition (%)	IC_{50} (µg/mL)
	Control	0.715		
Schiff base ligand, K(val-van)	25	0.728	3.56	2.43%
	50	0.690	9.76	
	75	0.681	11.01	
	100	0.646	14.00	
$[Sm(val\text{-}van)_2(H_2O)_3Cl]\cdot H_2O$	25	0.694	12.93	11.14%
	50	0.576	19.44	
	75	0.556	22.23	
	100	0.539	24.61	
$[Nd(val\text{-}van)_2(H_2O)_3Cl]\cdot H_2O$	25	0.548	23.35	19.17%
	50	0.533	25.45	
	75	0.502	29.79	
	100	0.490	31.46	
$[Dy(val\text{-}van)_2(H_2O)_3Cl]\cdot H_2O$	25	0.610	14.68	14.15%
	50	0.591	17.34	
	75	0.576	19.44	
	100	0.554	22.51	
Ascorbic acid	25	0.451	46.56	42.07%
	50	0.402	87. 36	
	75	0.400	90.02	
	100	0.395	93.12	

TABLE-5
ANTI-INFLAMMATORY ACTIVITY OF SCHIFF BASE LIGAND AND ITS LANTHANIDE COMPLEXES

Compounds	Concentration (µg)	OD at 416 nm	Inhibition (%)
	Control	1.052	
Schiff base ligand; K(val-van)	25	0.829	21.00
	50	0.801	23.85
	75	0.791	24.80
	100	0.782	25.66
$[Sm(val\text{-}van)_2(H_2O)_3Cl]\cdot H_2O$	25	0.748	28.89
	50	0.722	31.36
	75	0.698	33.65
	100	0.672	36.12
$[Nd(val\text{-}van)_2(H_2O)_3Cl]\cdot H_2O$	25	0.779	25.95
	50	0.762	27.56
	75	0.742	29.27
	100	0.728	30.79
$[Dy(val\text{-}van)_2(H_2O)_3Cl]\cdot H_2O$	25	0.776	26.20
	50	0.754	28.32
	75	0.732	30.41
	100	0.715	32.03

Antidiabetic activity: The compounds were evaluated for their antidiabetic efficacy by primarily assessing α-amylase

inhibition, contrasting the results with standard acarbose, as shown in Table-6. The antidiabetic activity at the concentration of 12.5, 25, 50, 100 and 200 µg/mL. The IC_{50} values of Schiff base ligand, Sm(III), Nd(III) and Dy(III) complexes were found to be 28.54, 35.07, 25.31 and 26.08%, respectively. The antidiabetic activity of the Nd(III) complex exhibited significant inhibitory effects compared to both the standard and the Schiff base ligand. This research emphasizes the development of new drugs, even for complex disorders like diabetes mellitus, given its global health impact. Schiff base metal complexes have shown promising insulin-mimetic qualities in various research studies addressing abnormal insulin production, the root cause of diabetes mellitus [51].

TABLE-6
ANTI-DIABETIC ACTIVITY OF SCHIFF BASE LIGAND AND ITS LANTHANIDE COMPLEXES

Compounds	Conc. (µg/mL)	OD at 540 nm	Inhibition (%)	IC_{50} (µg/mL)
	Control	0.2541		
Schiff base ligand	12.5	0.1792	29.4765	28.54%
	25	0.1688	33.5694	
	50	0.1628	35.9307	
	100	0.1536	39.5513	
	200	0.1497	41.0861	
[Sm(val-van)$_2$(H$_2$O)$_3$Cl]·H$_2$O	12.5	0.1632	35.7733	35.07%
	25	0.1578	37.8984	
	50	0.1514	40.4171	
	100	0.1428	43.8016	
	200	0.1402	44.8248	
[Nd(val-van)$_2$(H$_2$O)$_3$Cl]·H$_2$O	12.5	0.1848	27.2727	25.31%
	25	0.1715	32.5068	
	50	0.1636	35.6158	
	100	0.1578	37.8984	
	200	0.1432	43.6442	
[Dy(val-van)$_2$(H$_2$O)$_3$Cl]·H$_2$O	12.5	0.1836	27.7449	26.08%
	25	0.1782	29.8701	
	50	0.1732	31.8378	
	100	0.1626	36.0094	
	200	0.1512	44.4958	
Acarbose standard	12.5	0.1531	39.7481	38.26%
	25	0.1457	42.6604	
	50	0.1396	45.061	
	100	0.1263	50.2952	
	200	0.1175	53.7584	

Larvicidal activity: The larvicidal activity data of the compounds against *Culex quinquefasciatus* mosquito larvae are shown in Table-7. The synthesized Ln(III) complexes demonstrated a significant the larvicidal effect suggesting their potential as insecticidal agents for mosquito control. Specifically, the Nd(III) complex exhibited an increased mortality rate compared to the Schiff base ligand and the complexes, against the Culex mosquitoes.

TABLE-7
MORTALITY VALUES OF SCHIFF BASE LIGAND AND ITS LANTHANIDE COMPLEXES

Compounds	Larvicidal activity (%)			
	24 h	48 h	72 h	96 h
Schiff base ligand; K(val-van)	10	16	19	23
[Sm(val-van)$_2$(H$_2$O)$_3$Cl]·H$_2$O	10	16	22	25
[Nd(val-van)$_2$(H$_2$O)$_3$Cl]·H$_2$O	14	18	24	28
[Dy(val-van)$_2$(H$_2$O)$_3$Cl]·H$_2$O	12	18	20	26

Conclusion

The synthesis of Sm(III), Nd(III) and Dy(III) complexes with the Schiff base ligand derived from L-valine and vanillin by solid-state method was accomplished. The synthesized compounds were characterized by elemental analyses, molar conductivities, magnetic susceptibility, FT & FAR-IR, UV-Vis, NMR, ESI-MS spectra and thermal analyses. The ^{1}H NMR data suggested that the deprotonated phenolic oxygen after the complexation. In these complexes, the tridentate Schiff base ligand coordinated to Ln(III) ion through phenolic-oxygen, azomethine-nitrogen and carboxylate–oxygen atoms forming stable complexes, with a coordination number ten. The complexes display characteristic luminescence emissions from the central metal ions, attributed to efficient energy transfer from the Schiff base ligand to the metal center. Band gap measurements of 2.75, 2.64 and 2.69 eV for Sm(III), Nd(III) and Dy(III), respectively, fall within the semi-conducting range. Antioxidant activity assessment using a radical scavenging method shows that the Ln(III) complexes exhibit more effective antioxidant activity than the standard. Antimicrobial screening reveals higher activity for the Ln(III) complexes compared to the Schiff base ligand. In terms of anti-inflammatory activity, all the lanthanide(III) complexes exhibit significant inhibition of protein denaturation compared to the Schiff base ligand. The complexes also demonstrate good inhibitory activity for α-amylase. In larvicidal activity, the lanthanide(III) complexes show an increased mortality rate compared to the Schiff base ligand and display good activity against Culex mosquitoes. Also the synthesized lanthanide(III) complexes may serve as potential insecticidal substances in mosquito control. The study concludes that these lanthanide(III) compounds possess intriguing physical, chemical and potentially advantageous chemotherapeutic properties.

ACKNOWLEDGEMENTS

The authors are thankful to the authorities of SAIF, for giving technical support for the study.

CONFLICT OF INTEREST

The authors declare that there is no conflict of interests regarding the publication of this article.

REFERENCES

1. S.H. Sumrra, M. Ibrahim, S. Ambreen, M. Imran, M. Danish and F.S. Rehmani, *Bioinorg. Chem. Appl.*, **2014**, 812924 (2014); https://doi.org/10.1155/2014/812924
2. A.J. Al-Shaheen and M. Adil Al-Mula, *Kirkuk Uni. J Sci. Studies*, **10**, 127 (2015); https://doi.org/10.32894/kujss.2015.101965
3. I.P. Ejidike and P.A. Ajibade, *Bioinorg. Chem. Appl.*, **2016**, 9672451 (2016); https://doi.org/10.1155/2016/9672451
4. K.Y. El-Baradie, N.A. El-Wakiel and H.A. El-Ghamry, *Appl. Organomet. Chem.*, **29**, 117 (2015); https://doi.org/10.1002/aoc.3255
5. Y.H. Ebead, H.M.A. Salman, Y.M. Shebany and M.A. Abdellah, *Synth. React. Inorg. Met.-Org. Nano-Met. Chem.*, **46**, 1819 (2016); https://doi.org/10.1080/15533174.2011.617348

6. N. Saikumari, *Mater. Today Proc.*, **47**, 1777 (2021); https://doi.org/10.1016/j.matpr.2021.02.607
7. S. Kumari, Seema, P. Yadav, S. Sharma And M. Ranka, *Asian J. Chem.*, **34**, 2465 (2022); https://doi.org/10.14233/ajchem.2022.23757
8. H.L. Singh and J.B. Singh, *Int. J. Inorg. Chem.*, **2012**, 7 (2012); https://doi.org/10.1155/2012/568797
9. S. Alghool, H.F. Abd El-Halim, M.S. Abd El-sadek, I.S. Yahia and L.A. Wahab, *J. Therm. Anal. Calorim.*, **112**, 671 (2013); https://doi.org/10.1007/s10973-012-2628-4
10. B.A. Elsayed, I.A. Ibrahem, S.M. Shaaban and M.M. Elsenety, *Al Azhar Bull. Sci*, **25**, 9 (2014); https://doi.org/10.21608/absb.2014.23794
11. R.D. Teo, J. Termini and H.B. Gray, *J. Med. Chem.*, **59**, 6012 (2016); https://doi.org/10.1021/acs.jmedchem.5b01975
12. S. Alghool, M.S. Zoromba and H.F.A. El-Halim, *J. Rare Earths*, **31**, 715 (2013); https://doi.org/10.1016/S1002-0721(12)60347-0
13. S. Shahraki, F. Shiri, M. Heidari Majd and S. Dahmardeh, *J. Iranian Chem. Soc.*, **16**, 301 (2019); https://doi.org/10.1007/s13738-018-1508-7
14. J. Thomas and K.S. Ambili, *J. Mol. Struct.*, **1098**, 167 (2015); https://doi.org/10.1016/j.molstruc.2015.06.023
15. Z. Sulaiman, J. Naaliya and A.A. Umar, *Bayero J. Pure Appl. Sci.*, **12**, 638 (2019).
16. V. Anusuya, N. Murugananthan, P. Anitha and S. Mahesh, *Orient. J. Chem.*, **38**, 1525 (2022); https://doi.org/10.13005/ojc/380626
17. J.H. Van Vleck and A. Frank, *Phys. Rev.*, **34**, 1494 (1929); https://doi.org/10.1103/PhysRev.34.1494
18. M. Zhao, L. Wang, P. Li, J. Ma and W. Zheng, *Dalton Trans.*, **45**, 11172 (2016); https://doi.org/10.1039/C6DT00696E
19. W.J. Geary, *Coord. Chem. Rev.*, **7**, 81 (1971); https://doi.org/10.1016/S0010-8545(00)80009-0
20. M. Faye, P.A. Gaye, M.M. Sow, M. Dieng, F.B. Tamboura, N. Gruber and M. Gaye, *Earth. J. Chem. Sci.*, **6**, 99 (2021); https://doi.org/10.34198/ejcs.6121.99117
21. N. Gayathri, M.S. Suresh and V. Prakash, *Der Pharma Chem.*, **9**, 128 (2017).
22. K. Mohanan, N. Subhadrambika, R. Selwin Joseyphus, S.S. Swathy and V.P. Nisha, *J. Saudi Chem. Soc.*, **20**, 379 (2016); https://doi.org/10.1016/j.jscs.2012.07.007
23. N.S. Alahmadi and R.F.M. Elshaarawy, *J. Mol. Liq.*, **281**, 451 (2019); https://doi.org/10.1016/j.molliq.2019.01.154
24. L. Lekha, K. Kanmani Raja, G. Rajagopal and D. Easwaramoorthy, *J. Organomet. Chem.*, **753**, 72 (2014); https://doi.org/10.1016/j.jorganchem.2013.12.014
25. X. Zhang, Y. Zhang, L. Yang, R. Yang and D. Jin, *Synth. React. Inorg. Met.-Org. Chem.*, **30**, 45 (2000); https://doi.org/10.1080/00945710009351746
26. P. Jayaseelan, S. Prasad, S. Vedanayaki and R. Rajavel, *Arab. J. Chem.*, **9**, S668 (2016); https://doi.org/10.1016/j.arabjc.2011.07.029
27. C. Shiju, D. Arish and S. Kumaresan, *Spectrochim. Acta A Mol. Biomol. Spectrosc.*, **105**, 532 (2013); https://doi.org/10.1016/j.saa.2012.12.066
28. M. Thankamony, B.S. Kumari, G. Rijulal and K. Mohanan, *J. Therm. Anal. Calorim.*, **95**, 259 (2009); https://doi.org/10.1007/s10973-008-9116-x
29. E.M. Jincy, P.K. Rejimon and M.K.M. Nair, *Int. J. Appl. Adv. Sci. Res.*, **2**, 2456 (2017).
30. M.A. Mahmoud and M.G. Abou-Elmagd, *Egypt. J. Chem.*, **63**, 1009 (2020); https://doi.org/10.21608/ejchem.2019.13640.1858
31. N.M. Hosny and Y.E. Sherif, *Spectrochim. Acta A Mol. Biomol. Spectrosc.*, **136**, 510 (2015); https://doi.org/10.1016/j.saa.2014.09.064
32. R.K. Agarwal, H. Agarwal, S. Prasad and A. Kumar, *J. Korean Chem. Soc.*, **55**, 594 (2011); https://doi.org/10.5012/jkcs.2011.55.4.594
33. T.R. Rao, S. Shrestha, A. Prasad and K.K. Narang, *Synth. React. Inorg. Met.-Org. Chem.*, **32**, 419 (2002); https://doi.org/10.1081/SIM-120003216
34. V.F. Shulgin, O.V. Konnik, S.V. Abkhairova, A.N. Gusev, S.B. Meshkova, A.V. Kiriyak, E.B. Rusanov, M. Hasegawa and W. Linert, *Inorg. Chim. Acta*, **402**, 33 (2013); https://doi.org/10.1016/j.ica.2013.03.044
35. B. Cristovao and Z. Hnatejko, *J. Mol. Struct.*, **1088**, 50 (2015); https://doi.org/10.1016/j.molstruc.2015.01.032
36. R. Maouche, S. Belaid, B. Benmerad, S. Bouacida, S. Freslon, C. Daiguebonne, Y. Suffren, G. Calvez, K. Bernot, C. Roiland, L. Le Pollès and O. Guillou, *Inorg. Chim. Acta*, **501**, 119309 (2020); https://doi.org/10.1016/j.ica.2019.119309
37. N.H. Nasaruddin, S.Z. Ahmad, H. Bahron, N.M.M. Abd Rahman and N.S.M. Yusof, *Malaysian J. Chem.*, **23**, 91 (2021).
38. K.R. Joshi, A.J. Rojivadiya and J.H. Pandya, *Int. J. Inorg. Chem.*, **2014**, 17412 (2014); https://doi.org/10.1155/2014/817412
39. P. Yan, W. Sun, G. Li, C. Nie, T. Gao and Z. Yue, *J. Coord. Chem.*, **60**, 1973 (2007); https://doi.org/10.1080/00958970701217602
40. A. Pui, T. Malutan, L. Tataru, C. Malutan, D. Humelnicu and G. Carja, *Polyhedron*, **30**, 2127 (2011); https://doi.org/10.1016/j.poly.2011.05.029
41. L.F. Chu, Y. Shi, D.F. Xu, H. Yu, J.R. Lin and Q. He, *Synth. React. Inorg. Met.-Org. Nano-Met. Chem.*, **45**, 1617 (2015); https://doi.org/10.1080/15533174.2015.1031048
42. Y. Sindhu, C.J. Athira, M.S. Sujamol, R.S. Joseyphus and K. Mohanan, *Synth. React. Inorg. Met.-Org. Nano-Met. Chem.*, **43**, 226 (2013); https://doi.org/10.1080/15533174.2012.740711
43. H.L. Singh, *Main Group Met. Chem.*, **39**, 67 (2016); https://doi.org/10.1515/mgmc-2015-0039
44. I.T. Siraj and I.A. Sadiq, *ChemSearch J.*, **7**, 34 (2016).
45. Y.K. Vaghasiya, R. Nair, M. Soni, S. Baluja and S. Shanda, *J. Serb. Chem. Soc.*, **69**, 991 (2004); https://doi.org/10.2298/JSC0412991V
46. A.M. Ajlouni, Z.A. Taha, A.K. Hijazi and W.M.A. AlMomani, *Appl. Organomet. Chem.*, **32**, e4536 (2018); https://doi.org/10.1002/aoc.4536
47. J. Saranya, R.B. Priyadharsini and S.S. Lakshmi, *Int. J. Adv. Sci. Res.*, **12(03 Suppl 2)**, 118 (2021); https://doi.org/10.55218/JASR.s2202112314
48. T.F.A.F. Reji, A.J. Pearl and B.A. Rosy, *J. Rare Earths*, **31**, 1009 (2013); https://doi.org/10.1016/S1002-0721(13)60022-8
49. H.S. Abood, U.H. Ramadhan and H. Hamza, *Biochem. Cell. Arch.*, **20**, 5627 (2020).
50. A. Sharmila, P. Thamizhini and K.L. Prabha, *Rasayan J. Chem.*, **14**, 653 (2021); https://doi.org/10.31788/RJC.2021.1415935
51. M.N. Uddin, S.S. Ahmed and S.M.R. Alam, *J. Coord. Chem.*, **73**, 3109 (2020); https://doi.org/10.1007/s10534-008-9136-9